NONUNIFORM SAMPLING IN POLAR COORDINATES WITH APPLICATIONS TO COMPUTERIZED TOMOGRAPHY

Evgeny Margolis and Yonina C. Eldar

Department of Electrical Engineering
Technion – Israel Institute of Technology, Haifa, 32000, Israel
E-mail: margolis@tx.technion.ac.il, yonina@ee.technion.ac.il

ABSTRACT

We consider the problem of reconstructing a 2-D bandlimited signal from its nonuniform samples taken in polar coordinates. We introduce two nonuniform sampling strategies in polar coordinates and develop algorithms for reconstructing the signal from these samples. The proposed methods collect nonuniform samples along concentric circles or radial lines, where the circles or lines are nonuniformly distributed. We then apply these methods to the problem of reconstruction of tomographic images and show through simulations that they result in a higher quality of reconstruction with respect to the traditionally used algorithms.

1. INTRODUCTION

In most practical applications involving sampling of 2-D signals the standard rectilinear *Cartesian coordinate system* is used to represent the signal and its samples. However, by introducing *polar coordinates* one can simplify significantly the sampling and reconstruction methods. In particular, polar sampling strategies and linear spiral scan techniques, which are widely used in CT and MRI, provide practical advantages in the context of medical imaging [1]. While treatment with 2-D signals given in Cartesian coordinates is well developed both in theory and applications, the polar coordinate system is less understood and developed.

In this paper, we consider the problem of reconstruction of 2-D bandlimited signals from nonuniform samples given in polar coordinates. This problem was considered by Marvasti in [2], in which a reconstruction method was developed involving complex-valued functions. In this paper, we will show that reconstruction can be obtained using real valued functions that are simpler than those derived in [2].

In Section 2, we start with a brief introduction of the methods for reconstruction of 1-D periodic bandlimited signals from nonuniform samples. Since any function $f(r,\theta)$ given in polar coordinates is 2π-periodic in θ, in Section 3, we extend the 1-D results to the reconstruction of 2-D signals from nonuniformly spaced samples in polar coordinates. As an application of these results, we apply them in Section 4 to reconstruction of tomographic images from their frequency domain samples, which are usually taken in polar coordinates.

2. RECONSTRUCTION OF PERIODIC BANDLIMITED SIGNALS FROM NONUNIFORM SAMPLES

In this section, we present methods for reconstruction of 1-D periodic bandlimited signals from nonuniform, uniform, and recurrent nonuniform samples, which are fully adapted from [3]. These results will be used in Section 3 to establish two new theorems for reconstruction of 2-D functions nonuniformly sampled in polar coordinates.

We first note that a periodic signal $x(t)$, with period T, has a Fourier series representation $x(t)=\sum_{n=-\infty}^{\infty} c_n \exp(j2\pi nt/T)$ and Fourier transform $X(\omega)=\sum_{n=-\infty}^{\infty} c_n \delta(\omega-2\pi n/T)$, where $\delta(\omega)$ is the Dirac delta function. A T-periodic signal $x(t)$ is said to be bandlimited to $2\pi K/T$ if $c_n=0$ for $|n|>K$. It was proved in [3] that such a signal can be perfectly reconstructed from a finite number $N \geqslant 2K+1$ of its arbitrary spaced samples $x(t_p)$ as

$$x(t)=\sum_{p=0}^{N-1} x(t_p)h_p(t), \tag{1}$$

where

$$h_p(t)=\begin{cases} \prod_{\substack{q=0\\ q\neq p}}^{N-1} \frac{\sin(\pi(t-t_q)/T)}{\sin(\pi(t_p-t_q)/T)}, & N \text{ odd;} \\ \cos\left(\frac{\pi(t-t_p)}{T}\right) \prod_{\substack{q=0\\ q\neq p}}^{N-1} \frac{\sin(\pi(t-t_q)/T)}{\sin(\pi(t_p-t_q)/T)}, & N \text{ even.} \end{cases} \tag{2}$$

For the case of uniform samples the set of reconstruction function of (2) can be simplified to the form

$$h_p(t)=\begin{cases} \frac{\sin(N\pi(t-t_p)/T)}{N\sin(\pi(t-t_p)/T)}, & N \text{ odd;} \\ \cos\left(\frac{\pi(t-t_p)}{T}\right) \frac{\sin(N\pi(t-t_p)/T)}{N\sin(\pi(t-t_p)/T)}, & N \text{ even.} \end{cases} \tag{3}$$

For the case of recurrent nonuniform samples, where a group of N_r nonuniformly spaced points repeats itself M_r times with recurrent period T_r along the T-periodic signal, *i.e.*, $M_rT_r=T$, the reconstruction functions reduce to

$$h_p(t)=\begin{cases} b_p \frac{\prod_{q=0}^{N_r-1} \sin(M_r\pi(t-t_q)/T)}{\sin(\pi(t-t_p)/T)}, & N \text{ odd;} \\ b_p \cos\left(\frac{\pi(t-t_p)}{T}\right) \frac{\prod_{q=0}^{N_r-1} \sin(M_r\pi(t-t_q)/T)}{\sin(\pi(t-t_p)/T)}, & N \text{ even,} \end{cases} \tag{4}$$

where

$$b_p=\frac{1}{M_r \prod_{q=0,q\neq p}^{N_r-1} \sin(M_r\pi(t_p-t_q)/T)}. \tag{5}$$

As shown in [4], the reconstruction in both these cases, uniform and recurrent nonuniform, can be obtained using LTI filters. An alternative reconstruction algorithm, which results in more stable reconstruction of oversampled periodic signals in noisy environments, is developed in [5].

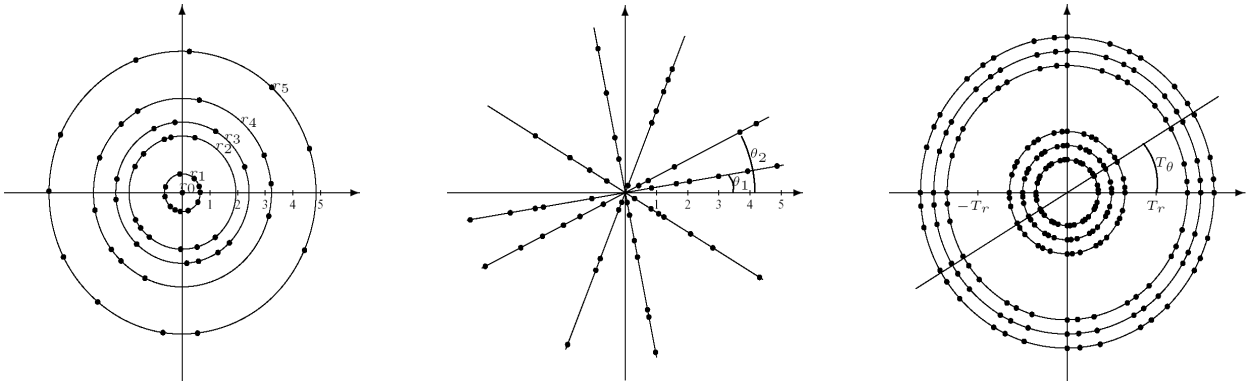

Fig. 1. Sampling strategies in polar coordinates.

3. SAMPLING IN POLAR COORDINATES

Butzer and Hinsen [6] considered reconstruction from nonuniform samples in 2-D cartesian coordinates, in which the nonuniform sampling points all lie on straight lines parallel to the y axis, and the average sampling density in both coordinates is greater than the Nyquist rate. As we show, Butzer's interpolation theorem can be extended to nonuniform sampling in polar coordinates, in which nonuniform samples lie either on concentric circles or on radial lines, where these circles or lines are nonuniformly distributed. Theorems 1 and 2 below exploit the 1-D results of Section 2 for reconstruction from nonuniform samples in the 2π-periodic azimuthal coordinate θ and Butzer's 1-D method for reconstruction from nonuniform samples in the non-periodic radial coordinate r.

3.1. First Sampling Strategy

In the first sampling method, we consider the signal $f(r,\theta)$, which is nonuniformly sampled along nonuniformly spaced circles. Theorem 1 below describes how and under which conditions the signal $f(r,\theta)$ can be perfectly reconstructed from this set of samples.

We first extend the function $f(r,\theta)$, which is given in polar coordinates $0 \leqslant \theta < 2\pi,\ r \geqslant 0$ to the function $\widetilde{f}(r,\theta)$, given by

$$\widetilde{f}(r,\theta) = \begin{cases} f(r,\theta), & r \geqslant 0; \\ f(-r,\theta+\pi), & r < 0. \end{cases} \tag{6}$$

The reason for this extension is the fact that for the interpolation process in the radial direction we need $-\infty < r < \infty$.

Theorem 1. *Let $\{r_n;\ n = 0,1,2\ldots\}$ be a sampling sequence of real numbers with average density greater than R/π, where each number corresponds to a circle with radius r_n centered at the origin. Let $\{\theta_{nm};\ n = 0,1,2,\ldots,\ m = 0,1,\ldots N-1\}$ be a set of real numbers, which defines nonuniform samples on the circle r_n, where $N \geq 2K+1$. If $\{r_n\}$ satisfies*

$$\begin{aligned} &|r_n - n\tfrac{\pi}{R}| < L < \infty, \\ &|r_n - r_k| > \delta > 0, \qquad n \neq k, \end{aligned} \tag{7}$$

then any function $f(r,\theta)$ bandlimited to the circular disc of radius R and angularly bandlimited to K can be perfectly reconstructed from this set of nonuniform samples by

$$f(r,\theta) = \sum_{n=-\infty}^{\infty} \sum_{m=0}^{N-1} \widetilde{f}(r_n,\theta_{nk}) \Phi_{nm}(\theta) \frac{G(r)}{G'(r_n)(r-r_n)}, \tag{8}$$

where

$$G(r) = (r-r_0) \prod_{\substack{n=-\infty \\ n\neq 0}}^{\infty} \left(1 - \frac{r}{r_n}\right) \tag{9}$$

and $\{\Phi_{nm}(\theta)\}_{m=0}^{N-1}$ are defined in (2) with $t=\theta$, $T=2\pi$, and $p=m$. Index n in $\Phi_{nm}(\theta)$ attributes the set of reconstruction functions to the azimuthal samples on a circle with radius r_n.

As an example of Theorem 1, any function $f(r,\theta)$ sampled with the pattern depicted in Fig. 1 (left) can be perfectly reconstructed from its samples, if its Fourier transform is radially bandlimited to a disc of radius $R=\pi$ and the highest harmonic of its Fourier series representation with respect to θ is $K=5$.

3.2. Second Sampling Strategy

In the second sampling strategy, the nonuniform samples all lie on nonuniformly spaced radial lines. We observe that the azimuthal samples form a set of recurrent nonuniform samples, where the set of $N/2$ nonuniform samples is repeated twice with period π. This fact simplifies the reconstruction in the θ coordinate.

Theorem 2. *Let $\{\theta_n;\ n = 0,1,\ldots N/2-1\}$ be a sequence of $N/2$ real numbers in the range $[0,\pi]$, where $N > 2K+1$. Let $\{r_{nm};\ m \in Z\}$ be a set of real numbers with average density greater than R/π, where each set defines nonuniform samples along the radial line θ_n. If $\{r_{nm}\}$ satisfies (7), then any function $f(r,\theta)$ bandlimited to the circular disc of radius R and angularly bandlimited to K can be perfectly reconstructed from these nonuniform samples and the reconstruction is given by*

$$f(r,\theta) = \sum_{n=0}^{N-1} \sum_{m=-\infty}^{\infty} \widetilde{f}(r_{nm},\theta_n) \frac{G_n(r)}{G_n'(r_{nm})(r-r_{nm})} \Phi_n(\theta), \tag{10}$$

where

$$G_n(r) = (r-r_{n0}) \prod_{\substack{m=-\infty \\ m\neq 0}}^{\infty} \left(1 - \frac{r}{r_{nm}}\right), \tag{11}$$

and $\{\Phi_n(\theta)\}_{n=0}^{N-1}$ are given in (4) with $t=\theta$, $T=2\pi$, $N_r = N/2$, $M_r = 2$, and $p=n$.

An example of the second sampling scheme is shown in Fig. 1 (middle), with five radial lines, *i.e.*, $N=10$, and the average

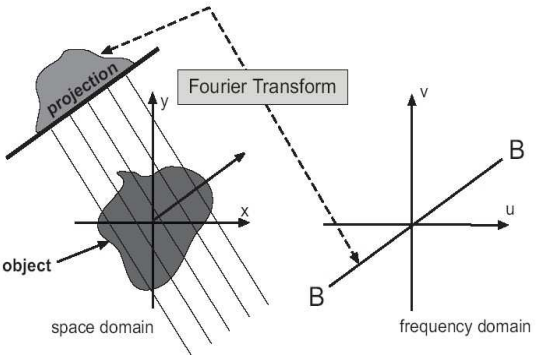

Fig. 2. Radon Transform and the Fourier Slice Theorem.

sampling density on each line is greater than one. Thus, any function $f(r,\theta)$ can be perfectly reconstructed from these nonuniform samples, if its Fourier transform is bandlimited to a disc of radius $R=\pi$ and angularly bandlimited to $K=4$.

We note that in [2] Marvasti also considered the problem of reconstruction from nonuniform samples in polar coordinates. The interpolation functions he developed involve complex-valued functions, and are therefore more complicated to implement. Our methods, developed in this section, are more efficient but are still computationally difficult. In [3], an efficient implementation of these reconstruction methods with LTI filters is developed for uniform and recurrent nonuniform sampling along both coordinates. Such a sampling structure is presented in Fig. 1 (right), where we perform recurrent nonuniform sampling along each of the coordinates r and θ.

In the next section, we present an application of the reconstruction methods developed in this section, to CT.

4. TOMOGRAPHIC IMAGE RECONSTRUCTION

4.1. Principals of Computerized Tomography

Computerized tomography is a method for reconstructing a multidimensional signal from its projections, taken from different angles in a lower dimensional space [7]. In parallel beam tomography, a series of parallel rays of high-frequency radiation (usually in the X-ray spectrum) traverse the object $f(x,y)$. These rays of initial energy are attenuated by the object as they traverse across until they reach the detector on the other side (see Fig. 2 (left)). The remaining energy forms the *projection*, which can be expressed as line integral along a beam of parallel rays

$$P_\theta(r)=\iint_{\mathbb{R}^2} f(x,y)\delta(x\cos\theta+y\sin\theta-r)dxdy, \qquad (12)$$

where $f(x,y)$ is a 2-D function, space-limited to the circular disc of radius A. The function $R(\theta,r)=P_\theta(r)$ is called the *Radon transform* of the object $f(x,y)$ [8]. A fundamental tool of straight ray tomography is the *Fourier Slice Theorem*, which relates the 1-D Fourier transform of the projections and the 2-D Fourier transform of the object image:

Fourier Slice Theorem: The 1-D Fourier transform of the Radon transform $P_\theta(r)$ with respect to r gives a slice $S_\theta(\rho)$ of the 2-D Fourier transform $F(u,v)$ of the object, subtending an angle θ with the u-axis. In other words, the Fourier transform of a projection in Fig. 2 (left) gives the values of $F(u,v)$ along the line BB in Fig. 2 (right).

If an infinite number of projections are taken, then $F(u,v)$ would be known at all points in the $u-v$ plane and the function $f(x,y)$ can be recovered by using the inverse Fourier transform

$$f(x,y)=\int_{-\infty}^{\infty}\int_{-\infty}^{\infty} F(u,v)e^{j2\pi(ux+vy)}dudv. \qquad (13)$$

Using the fact that $f(x,y)$ is zero outside the region $Q=[-A,A]\times[-A,A]$, (13) can be written as

$$f(x,y)=\frac{1}{A^2}\sum_{m=-\infty}^{\infty}\sum_{n=-\infty}^{\infty} F\left(\frac{m}{A},\frac{n}{A}\right)e^{j2\pi(mx+ny)/A} \qquad (14)$$

for $[x,y]\in Q$. From (14) we conclude that if the function $F\left(\frac{m}{A},\frac{n}{A}\right)$ is known for all n and m, then $f(x,y)$ can be perfectly reconstructed. However, this condition does not hold in practice.

In real applications, the number of projections $P_\theta(r)$ is finite and form a discrete version of the Radon transform of the object. In that case the function $F(u,v)$ is only known along a finite number of radial lines. Moreover, the fact that a detector can detect only a finite number of parallel rays makes exact calculation of a slice $S_\theta(\rho)$ of $F(u,v)$ impossible. In the next section we discuss and propose a solution to the practical limitation of the method.

4.2. Reconstruction Method and Simulations

We now approximate the discrete version of $S_\theta(\rho)$ from the finite number of samples of the projection $P_\theta(r)$. For practical purposes, we may assume that each projection is bandlimited to W, *i.e.,* $S_\theta(\rho)=0$ for $|\rho|\geq W$. In this case, the projections can be sampled at intervals of $1/2W$, *i.e.,* W is determined by the distance between the sensors. Since the projections are also limited to $2A$, we have

$$P_\theta\left(\frac{m}{2W}\right), \quad m=-\frac{N_\rho-1}{2},\cdots,0,\cdots,\frac{N_\rho-1}{2}, \qquad (15)$$

where $N_\rho=\lfloor 4WA+1\rfloor$. Here $\lfloor\cdot\rfloor$ denotes the floor operator, which rounds down to the nearest integer. We then approximate the $S_\theta(\rho)$ at the finite number of points by the discrete Fourier transform of the projection

$$S_\theta\left(\frac{2Wm}{N_\rho}\right)\approx\frac{1}{2W}\sum_{k=-(N_\rho-1)/2}^{(N_\rho-1)/2} P_\theta\left(\frac{k}{2W}\right)e^{-j2\pi mk/N_\rho}. \qquad (16)$$

From (16) we conclude that we are given only a finite number of samples of $F(v,u)$ on the polar grid. In order to utilize (14), an interpolation has to be carried out to fill the Cartesian grid. This polar-cartesian interpolation is called *gridding*. It is common to determine the values on the square grid by some kind of *nearest-neighbor* or *linear interpolation* from the radial points [7]. These simple polar-cartesian interpolations may introduce inaccuracies to the reconstructed image. Therefore, accurate interpolation methods are required.

In our method, we propose using the reconstruction methods developed in Section 3 for polar-cartesian interpolation of $F(u,v)$

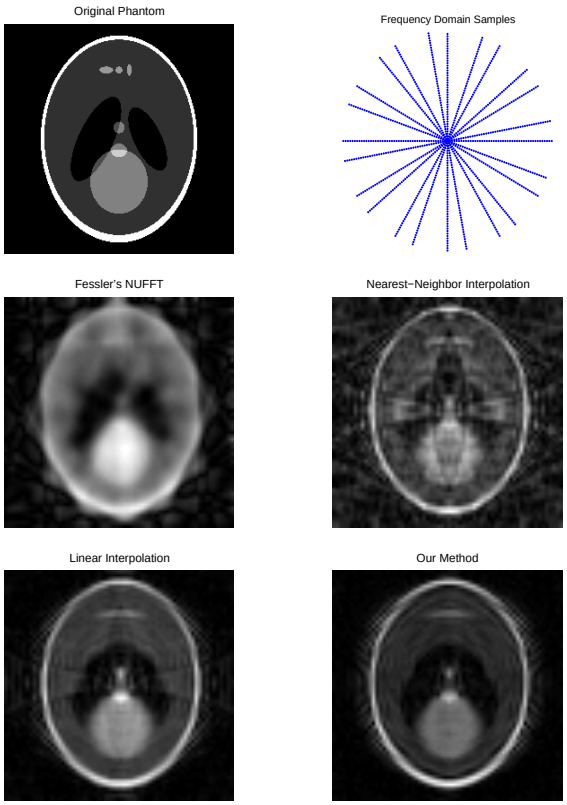

Fig. 3. Reconstruction of a Shepp-Logan phantom.

from its samples (16) given on a polar grid. We first note that the problem of reconstructing a 2-D signal bandlimited in the frequency domain and the problem of reconstructing the 2-D Fourier transform of a space-limited signal are mathematically equivalent. We also observe that the frequency domain samples of the reconstructed object in CT correspond to the second sampling strategy presented in Section 3.2, where samples of the 2-D signal all lie on radial lines passing through the origin. Therefore, relying on Theorem 2 and assuming that the Fourier transform $F(\rho, \theta)$ of the reconstructed image, which is given in polar coordinates, has a limited number of harmonics with respect to the θ coordinate, we have

$$F(\rho,\theta) = \sum_{n=0}^{N_\theta-1} \sum_{k=0}^{N_\rho-1} S_{\theta_n}(\rho_k)\Psi_k(\rho)\Phi_n(\theta), \qquad (17)$$

where $\Psi_k(\rho)$ and $\Phi_n(\theta)$ are defined in (3) and (4), respectively. Here the finite number of samples $\{S_{\theta_n}(\rho_k)\}_{k=0}^{N_\rho-1}$ on each radial line are periodically expanded with respect to the ρ coordinate and then the ideal $\mathrm{sinc}(\rho)$ interpolation is replaced by $\Psi_k(\rho)$ of (3). Although the Fourier transform of most functions of CT will not be angularly bandlimited, in practice the energy contained above a certain frequency can be negligible. Given the fully reconstructed Fourier transform $F(\rho, \theta)$ of an image $f(x, y)$ we resample it on the uniform grid, which is required in (14) for the IFFT calculation.

We now compare the proposed reconstruction algorithm to several methods, which are widely used for the reconstruction of tomographic images. Specifically, we consider *nearest-neighbor* and *linear interpolations* and *Fessler's NUFFT* [9], which exploits iterative algorithm for reconstruction of $f(x, y)$ from its frequency domain samples (16). Computer simulations illustrating performance of these methods are demonstrated for the well-known Shepp-Logan head phantom, which is presented in Fig. 3 (top-left).

Example: We consider the problem of reconstructing a Shepp-Logan head phantom from 12 recurrent nonuniform projections with $N_\rho = 91$ samples each. This set of samples is presented in Fig. 3. We note that uniform distribution in both coordinates is the most common in the context of CT images. However, projections can be nonuniformly distributed due to synchronization problems in the scanner machine. For instance, the set of projections considired in this example was generated by throwing out every third projection from the uniform set of 18 projections.

In Fig. 3, we present the original Shepp-Logan head phantom and four reconstructions obtained with different methods. We can clearly see that the reconstructed phantom is closer to the original when the method (17) proposed in this section is used for polar-cartesian gridding. From Fig. 3 we conclude that polar-cartesian gridding is very sensitive to the method used for interpolation and simple nearest-neighbor and linear techniques methods do not perform well and introduce artifacts in the reconstruction. We also observe that Fessler's NUFFT algorithm is not capable to recover the sharp edges and small objects of a Shepp-Logan head phantom. This iterative algorithm requires more frequency domain samples to reach the same quality achieved by our method.

5. REFERENCES

[1] H. Stark, "Polar, spiral and generalized sampling and interpolation," in *Advanced Topics in Shannon Sampling and Interpolation Theory*, R. J. Marks II, Ed., pp. 185–218. New York: Springer-Verlag, 1993.

[2] F. Marvasti, "Extension of Lagrange interpolation to 2-D signals in polar coordinates," *IEEE Trans. Circuits Syst.*, vol. 37, pp. 567–568, Apr. 1990.

[3] E. Margolis, "Reconstruction of periodic bandlimited signals from nonuniform samples," M.S. thesis, Technion–Israel Institute of Technology, June 2004.

[4] E. Margolis and Y. C. Eldar, "Filterbank reconstruction of periodic signals and sampling in polar coordinates," *Proceedings of the 2003 Workshop on Sampling Theory and Applications, SampTA'03*, May 2003.

[5] E. Margolis and Y. C. Eldar, "Reconstruction of nonuniformly sampled periodic signals: Algorithms and stability analysis," submitted to *Int. Conf. Electronics, Circuits and Systems (ICECS-2004)*.

[6] P. L. Butzer and G. Hinsen, "Two-dimensional nonuniform sampling expansions - An iterative approach I,II," *Appl. Anal.*, vol. 32, pp. 53–85, 1989.

[7] A. C. Kak and M. Slaney, *Principles of Computerized Tomographic Imaging*, SIAM, 2001.

[8] R. Deans, *The Radon Transform and Some of its Applications*, 1986.

[9] J. A. Fessler and B. P. Sutton, "Nonuniform fast Fourier transforms using min-max interpolation," *IEEE Trans. Signal Processing*, vol. 51, no. 2, pp. 560–574, Feb. 2003.